Large-Area Graphene Films by Simple Solution Casting of Edge-Selectively Functionalized Graphite

Seo-Yoon Bae,[†] In-Yup Jeon,[†] Jieun Yang,[†] Noejung Park,[†] Hyeon Suk Shin,[†] Sungjin Park,[‡] Rodney S. Ruoff,[§] Liming Dai,[⊥] and Jong-Beom Baek[†,*]

[†]Interdisciplinary School of Green Energy and Institute of Advanced Materials and Devices, Ulsan National Institute of Science and Technology (UNIST), 100, Banyeon, Ulsan 689-798, South Korea, [‡]Department of Chemistry, Inha University, Incheon 402-751, South Korea, [§]Department of Mechanical Engineering, The University of Texas at Austin and the Texas Materials Institute, Austin, Texas 78712, United States, and [⊥]Department of Macromolecular Science and Engineering, Case Western Reserve University, 10900 Euclid Avenue, Cleveland, Ohio 44106, United States

ABSTRACT We report edge-selective functionalization of graphite (EFG) for the production of large-area uniform graphene films by simply solution-casting EFG dispersions in dichloromethane on silicon oxide substrates, followed by annealing. The resultant graphene films show ambipolar transport properties with sheet resistances of 0.52−3.11 kΩ/sq at 63−90% optical transmittance. EFG allows solution processing methods for the scalable production of electrically conductive, optically transparent, and mechanically robust flexible graphene films for use in practice.

KEYWORDS: edge-selective functionalization · graphene film · solution processing · annealing · sheet resistance · optical transmittance

Exfoliation of graphite, including into individual layers (graphene), is of great interest due to the exceptional mechanical strength,[1] thermal conductivity,[2] and electronic properties[3] characteristics of graphene platelets. As a result, graphene is attractive for a wide range of potential applications in composites,[4] energy related systems,[5] sensors,[6] and others.[7−9] Graphene is a promising material for replacing indium tin oxide (ITO) in transparent conductive flat panels.[10] Currently, ITO is widely used as the transparent electrode in flat panel displays, because it has a relatively high electrical conductivity and optical transmittance with a very good stability to moisture and harsh environmental conditions.[11] However, indium is expensive and has a limited reserve in nature. In addition, ITO is not appropriate for flexible display devices due to limitations in its mechanical and optical properties. Recently, Hong *et al.* have demonstrated the feasibility for the use of large-area graphene films as the transparent conductor in flexible polymer film-based flat panel electronics.[12] These graphene films were grown on nickel (Ni)[10] and copper (Cu)[12,13] substrates at 1000 °C under a reduced pressure by chemical vapor deposition (CVD) process and then transferred onto polymer films. Unfortunately, these methods are not sufficiently cost and time effective to be commercially viable for mass production.[14] To meet commercial demands, new materials or processing methods would be essential. In this regard, graphene oxide (GO) has been investigated as a chemical alternative for mass production of graphene films by solution-based processes.[15] However, GO has poor quality and requires reduction, which has a limited conversion to reduced graphene oxide (rGO).[16] Hence, the original graphene structure from GO cannot be efficiently restored.

Here, we report the formation of large-area, flexible, conductive, and transparent graphene films *via* a simple solution casting of exfoliated platelets from edge-selectively functionalized graphite (EFG). The newly developed edge-selective functionalization method enabled us to achieve exfoliation of "pristine" graphite into individual graphene and few-layer graphene platelets in a scalable and simple manner.[17] For example, most of the 4-substituted benzoic acids can be used as "molecular wedges" and covalently attached to the edge of graphite. The edge groups on graphite are mainly sp^2-bonded C−H groups, a reactive site for "direct" Friedel−Crafts acylation in polyphosphoric acid (PPA)/phosphorus pentoxide (P_2O_5).

RESULTS AND DISCUSSION

From the elemental analysis (Supporting Information, Table S1), the possible available sp^2−bonded C−H sites at the edges could be calculated to be about one per every 45 carbons. Hence, a sufficient number

* Address correspondence to jbbaek@unist.ac.kr.

Received for review March 22, 2011 and accepted May 17, 2011.

Published online May 17, 2011
10.1021/nn201072m

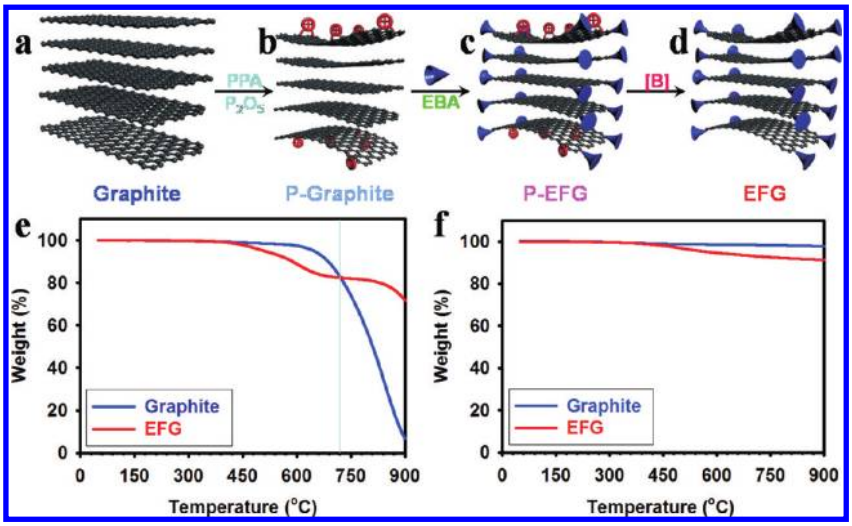

Figure 1. (a–d) Functionalization of 4-ethylbenzoic acid (EBA) onto the edge of "pristine" graphite in polyphosphoric acid (PPA)/phosphorus pentoxide (P_2O_5) to produce edge-selectively functionalized graphite (EFG). P-graphite, P-EFG and [B] stand for protonated graphite, protonated EFG, and base treatment, respectively. TGA thermograms obtained with a heating rate of 10 °C/min (e) in air; (f) in nitrogen. In order to exclude kinetic effect, TGA thermograms obtained with a heating rate of 1 °C/min in air are presented in Supporting Information, Figure S3.

of "wedge" molecules necessary for exfoliation can be attached around graphite by treating it with 4-ethylbenzoic acid (EBA) in the reaction medium PPA/P_2O_5 at 130 °C (Figure 1a–c). The EFG was then completely worked-up and analyzed (Figure 1d, see Methods, Supporting Information, Figures S1 and S2a) prior to dispersing in organic solvents.

Thermogravimetric analysis (TGA) was used to determine the amount of EBA grafted onto the graphite. As can be seen in Figure 1e, graphite is thermo-oxidatively stable up to 650 °C in air, while the EFG shows stepwise weight losses. We assign the first weight loss at about 400 °C, which continues until about 720 °C, to the EBA moiety being thermally "stripped off". Hence, the degree of functionalization can be quantified by the weight loss of EFG up to about 720 °C and it is approximately 15 wt %. The degree of functionalization was 76.5% of the available sp^2 bonded C–H sites. The temperature where the second weight loss starts is approximately 850 °C, or 200 °C higher than that of pristine graphite (650 °C), suggesting that carbon cations, anions, and/or radicals generated during heating (charring) of the 4-ethylbenzoyl (EB) moiety at the edges of EFG provide an *in situ* carbon feedstock for "healing" inherent defects on graphite and/or "edge-welding" (cross-linking) graphene platelets.[18] The high char yield (91 wt %) of EFG at 720 °C in a nitrogen atmosphere (Figure 1d) was much higher than that in dry air (85 wt %), suggesting that the formation of large-area graphene films could be possible *via* solution casting and subsequent "edge-welding" by thermal annealing at elevated temperature. To evaluate whether the "char" at the edges blocks oxidants from accessing the interior of the EFG, and hence keeps the graphitic plane structure intact, TGA thermograms were obtained with a ramp rate of 1 °C/min (Supporting Information, Figure S3). The thermograms for both graphite and EFG were very similar to those obtained with a ramp rate of 10 °C/min (see Figure 1e). Both samples had degradation temperatures down-shifted approximately 180 °C and the stepwise weight loss of mass in the EFG was evident leaving almost the same amount of char yield (15 wt %) at the plateau region at 540 °C. Hence, the higher thermo-oxidative stability of EFG after charring of the EBA moiety is not due to blocking of the oxidant (kinetic effect). More importantly, the fact that there is no weight loss around 100–200 °C, characteristic of interlamellar water in graphite oxide due to its hygroscopic nature,[19] strongly suggests that the graphite is not oxidized during the edge-functionalization in a mild PPA/P_2O_5 medium.

The covalently linked edge groups provide steric repulsion to open pristine graphite edges (Figure 2a) and thus, the EFG in solid state should consist of many stacks of graphene layers as schematically shown in Figure 2b. The partially edge-delaminated EFG allows efficient solvent penetration for the further exfoliation of EFG into few-layer graphene platelets and graphene in solution (Figure 2c). Wide-angle X-ray diffraction (XRD) patterns (Supporting Information, Figure S4) were applied to the same amount of pristine graphite, PPA/P_2O_5-treated graphite, and EFG to estimate the degree of exfoliation and functionalization of the basal plane; the peak intensity of EFG in the solid state is 10% of that of the precursor graphite with almost the same peak location at 26.58° (0.333 Å), indicating the efficient dispersion in solvents through a kind of "unzipping" mechanism schematically shown in Figure 2a–c and without basal plane functionalization. In a control

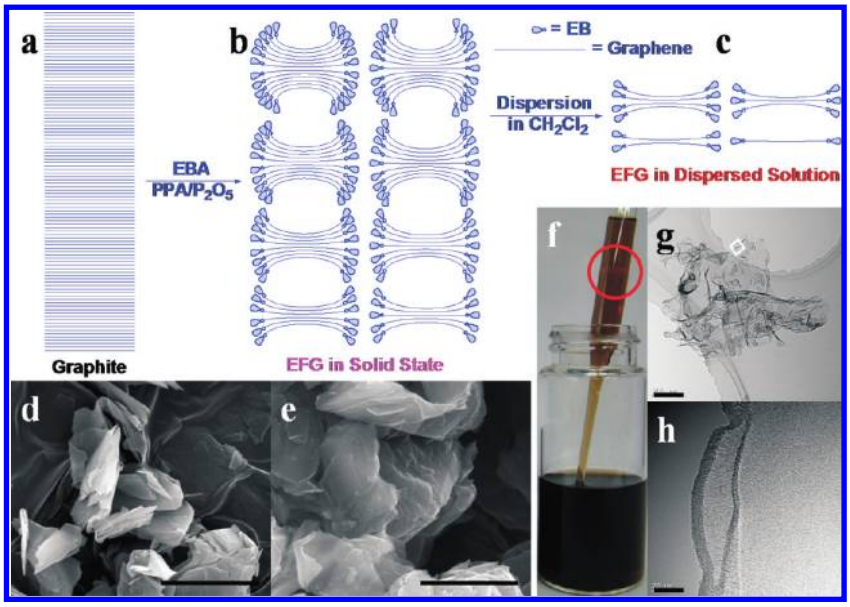

Figure 2. (a) Schematic presentation of pristine graphite. (b) Idealized structure of edge-functionalized graphite (EFG) in solid state. (c) Idealized structure of EFG in dispersed solution. (d) SEM image of pristine graphite (50000×). (e) SEM image of EFG (50000×) in solid state. Scale bars are 2 μm. (f) EFG-dispersed solution in dichloromethane. (g) TEM image of EFG on holey carbon grid. The thin EFG platelets are wrinkled and crumpled due to their flexibility. Scale bar is 200 nm. (h) TEM image of "edge-on" view, suggestive of edge functionalization at higher magnification from square in panel a. Scale bar is 20 nm.

experiment, graphite was exposed to the same reaction conditions used for the EFG synthesis in the absence of EBA to test if the reaction medium PPA/P_2O_5 could damage (oxidize) graphite. XRD patterns show that the peak intensity of PPA-treated graphite is stronger than that of graphite with the same peak location at 26.50° (0.334 Å) (Supporting Information, Figure S4). This implies that the PPA-treated graphite is not chemically altered but has increased crystallinity by selectively etching off of amorphous carbon attached to the surface of graphite. Further evidence for the structural integrity of the EFG basal plane region comes from the elemental (EA, Supporting Information, Table S1) and XPS (Figure S5) analyses, which revealed that there was no additional oxygen content beyond the value calculated on the basis of yield from the edge-selective functionalization. Scanning electron microscopy (SEM) of the precursor graphite powder shows that its surfaces are "clean and smooth" (Figure 2d), while the SEM image of bulk EFG in solid state shows fuzzier surfaces (Figure 2e), indicating that the attachment of EBA expanded the edge. Indeed, EFG is an ideal precursor (Figure 2b) for further exfoliation into scalable and high-quality individual graphene and few layer graphene platelets (Figure 2c).

The exfoliation/dispersibility of EFG was tested at room temperature in various solvents, namely water, methanol, ethanol, acetic acid, toluene, *N,N*-dimethylacetamide (DMAc), heptane, acetone, benzene, dichloromethane, tetrahydrofuran (THF), pyridine and *N*-methyl-2-pyrrolidone (NMP) (Supporting Information, Figure S2c). It was found that the EFG could be dispersed in all of these solvents, and among them the dispersions in dichloromethane yielded the highest concentration at room temperature. Without physical agitation of any kind (*e.g.*, it is known that sonication of certain types can damage the carbon framework[20]), the EFG was readily exfoliated to achieve stable dispersions with concentrations as high as 0.8 mg/mL in dichloromethane (Supporting Information, Figure S2c and Movie). Mechanical (magnetic) stirring favored more rapid dispersion. The amount of EFG dispersed in each solvent was calculated as described in the experimental section (see Methods). The maximum concentration for a long-term (months) stable dispersion achieved is 8× higher than that reported for dispersions of graphite (0.1 mg/mL) in NMP,[21] which was found to be stable only for days after sonication (see below). Unlike aqueous dispersions of graphite oxide (light yellow),[22] the color of the EFG dispersion in dichloromethane is dark brown due to high conjugation in the undamaged basal planes (Figure 2f and Supporting Information, Figure S2d). Tyndall scattering (red circle, Figure 2f) was observed with a hand-held laser pointer, demonstrating formation of colloid. After several months of standing in ambient condition, the supernatant from the dichloromethane dispersion at 0.8 mg/mL concentration remained visually unchanged with no sedimentation evident to the eye. On the other hand, the dispersion of graphite in NMP was readily separated,[21] indicating that the dispersion was not thermodynamically stable leaving an essentially clear liquid after 1 day (Supporting Information, Figure S2e). Molecular dynamics simulations suggest that the good dispersibility is because the phenyl rings on the EB groups are vertically aligned to the graphene

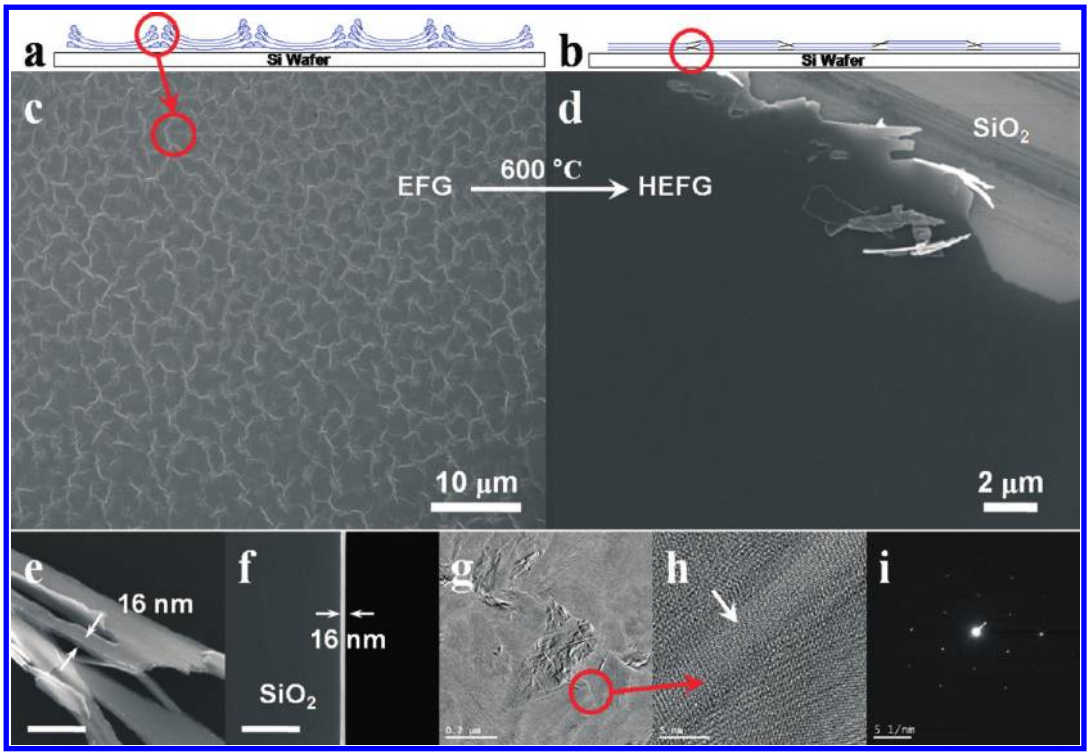

Figure 3. (a) Schematic presentation of as-cast EFG film on SiO_2 surface. (b) Schematic presentation of heat-treated EFG (HEFG) film on SiO_2 surface. (c) SEM image of as-cast EFG film drop-coated on SiO_2 surface from dichloromethane solution and then dried. (d) SEM image obtained on the surface of HEFG film at 600 °C under argon atmosphere for 3 h. The peeled-off area was scratched with a sharp metal tip, and this allowed discriminating the very smooth film from the SiO_2 surface substrate. (e) Edge-on SEM image of peeled-off area of HEFG film. Scale bar is 300 nm. (f) SEM image of the fracture surface of HEFG film on an SiO_2 surface. Scale bar is 300 nm. (g) TEM image of the surface of HEFG film. (h) TEM image focused on junction of HEFG at high magnification. (i) Selected area electron diffraction (SAED) pattern of HEFG film.

plane, leading to a strong steric hindrance for reaggregation of the dispersed graphene platelets (Supporting Information, Figure S6 and detailed computation conditions are described in the Methods section). Transmission electron microscope (TEM) images show the presence of graphene platelets (Figure 2g) with functionalized edges (Figure 2h).

The SEM image of a solution-cast EFG film deposited on silicon oxide (SiO_2, 300 nm) surface from a diluted solution in dichloromethane shows individualized EFG platelets, as schematically illustrated in Supporting Information, Figure S7a. The lateral width distribution of EFG platelets (Figure S7b) was determined by an image analyzer to be in the range of 0.2−2.2 μm (Figure S7c); the average lateral size was approximately 1.0 μm. AFM images of platelets, deposited from EFG further diluted in dichloromethane on an SiO_2 surface, were used to estimate thicknesses of the platelets (Supporting Information, Figure S8). The maximum heights of few-layer graphene platelets are in the range of 1.2−5.0 nm. As a result of the edge functionalization with EBA, the edge of EFG is not as sharp as graphene obtained from micromechanical exfoliation[23] or of reduced graphene oxide (rGO) platelets.[21] Together with Raman spectroscopy (Supporting Information, Figure S9a) and confocal optical microscopy image (Figure S9b), the object shown at the edge of the EFG platelet in Figure S8a is interpreted to be a few-layer EFG with its edge higher than its interior due to the presence of EB moieties at the edge.[24] The height profiles of platelets indicate that the maximum thickness of such platelets is less than 5 nm (Figure S8). The average lateral width from many other AFM images is ~1.0 μm. The width distribution from the AFM imaging agrees with the SEM result (see Figure S7).

The concentrated EFG dispersion in dichloromethane was drop-coated on an SiO_2 surface. The SEM image shows platelets on the surface over a large area with many wrinkles (Figure 3c), as depicted in a schematic illustration shown in Figure 3a. The as-cast film shows high sheet resistance (~108 kΩ/sq) likely due to the edge groups at the boundaries between platelets contributing high contact resistance. Upon heat treatment at 600 °C in argon for 3 h, the edge EB moieties could act as an *in situ* feedstock for carbon to "weld" the graphene platelets thus forming a large-area graphene film (Figure 3b, see also Supporting Information, Figure S10). Indeed, the SEM image of the heat-treated EFG (HEFG) film shows a uniform surface (Figure 3d). This film was scratched with a sharp metal (Figure 3d, see also Supporting Information, Figure S10a). The thickness of the HEFG film was determined to be 16 nm by SEM images (Figure 3e,f) and AFM images using tapping mode (Supporting Information,

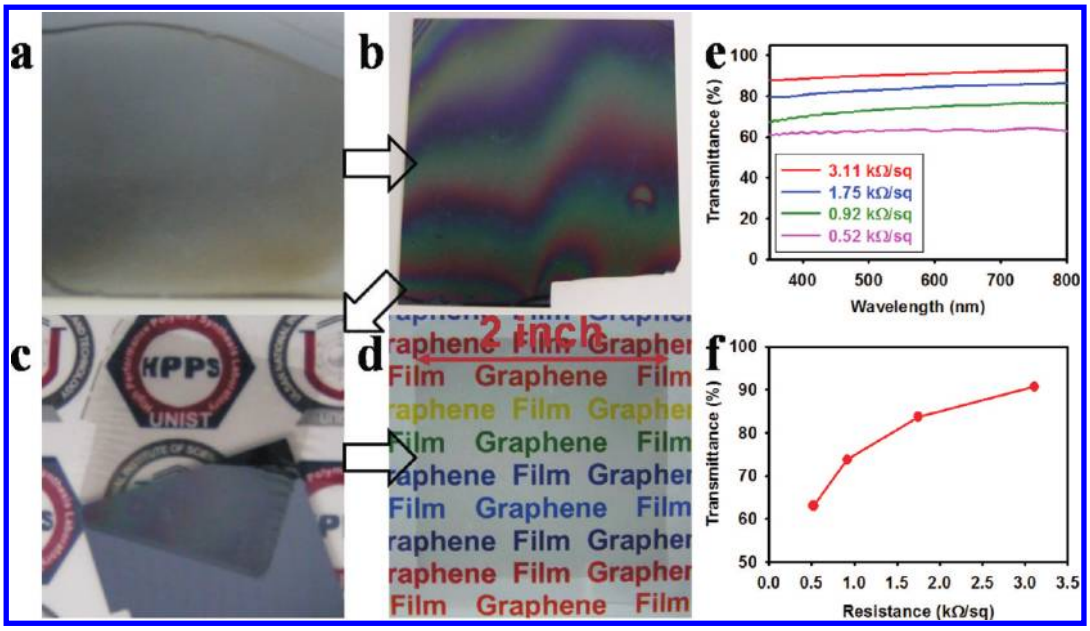

Figure 4. (a) Photograph of HEFG film on SiO_2 surface; (b) photograph of PMMA spin-coated on HEFG (HEFG/PMMA) film by spin coating; (c) freestanding HEFG/PMMA after SiO_2 surface eching; (d) 2 in. by 2 in. HEFG on PET (HEFG/PET) film; (e) optical transmittance with respect to wavelength; (f) transmittance *vs* sheet resistance curve.

Figure S10c). Welded boundaries of HEFG could be distinguished from the surface of HEFG thin film (red circle, Figure 3g). The boundary of platelets, where thermal welding was assumed to occur during heat-treatment, can be clearly seen at high magnification (Figure 3h). Selected area electron diffraction (SAED) indicates that the HEFG film has high crystallinity (Figure 3i). These results demonstrate that large-area graphene films can be achieved by solution casting. The 16 nm thick film had an average sheet resistance of 1.3 kΩ/sq. This value is a few orders of magnitude lower than that of the chemically rGO.[25,26] The observed reduction in sheet resistance through heating the EFG film supports the concept of edge chemistry "boundary welding" that is in a good agreement with the TGA results (see Figure 1b,c).[18]

Large-area graphene films were made with different EFG concentrations in dichloromethane. These solutions were drop-coated onto an SiO_2 surface and subsequently heat-treated at 600 °C in argon for 3 h (Figure 4a). To transfer the solution-cast HEFG films onto other substrates, poly(methylmethaacrylate) (PMMA) solution in tetrahydrofuran (THF) was spin coated on such a HEFG film (Figure 4b). The SiO_2 layer was etched off by floating on aqueous 1 M hydrofluoric acid (HF) solution (Figure 4c). Then, the HEFG on PMMA (HEFG/PMMA) film was transferred to poly(ethylene terephthalate) (PET) film and the PMMA was washed off by immersing in acetone to produce HEFG on PET (HEFG/PET) (Figure 4d). Four different HEFG/PET films with approximately 2 × 2 in. dimensions were tested, though many larger HEFG films on various substrates can be readily prepared through the similar procedure.

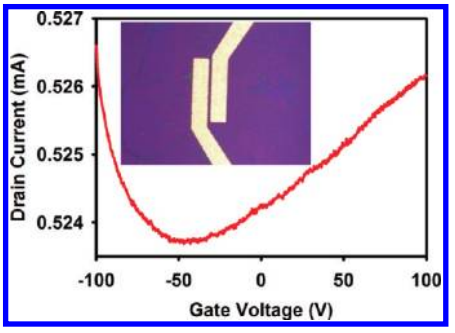

Figure 5. $I-V_g$ curve of a field-effect transistor of HEFG film. The measurement was carried out in vacuum and bias voltage between source and drain electrodes was 0.1 V. The inset is an optical microscopy image of the device with the channel length of 4 μm.

The optical transmittances and sheet resistances of the films were measured by using UV−vis spectroscopy and four-point probe, respectively. The optical transmittances are in the range of 63−90% (Figure 4e) with sheet resistances of 0.52−3.11 kΩ/sq (Figure 4f). Although these optoelectronic properties are still not as good as those of the CVD grown graphene film,[12] solution casting has many advantages in processing over the CVD process, indicating cost and scalability to very large area. Figure 5 shows *I*−*V* characteristics of a field-effect transistor of HEFG film that was transferred onto an SiO_2(300 nm)/Si wafer with prepatterned gold electrodes. The film shows ambipolar behavior with a Dirac point around −50 V.[27]

CONCLUSION

Edge-selectively functionalized graphite (EFG) without damage to the basal plane can be produced with a

simple one-pot reaction between graphite and 4-ethylbenzoic acid (EBA) in viscous PPA/P_2O_5 under mild conditions. The EFG could be dispersed in various organic solvents. Among 13 different organic solvents tested in this study, dichloromethane, THF, DMAc, and NMP were good solvents for dispersing EFG and this is attributed to high chemical affinity with these solvents. The EFG was dispersed in dichloromethane and exfoliated into EFG thin platelets. Edge-selective functionalization provides a pathway to exfoliation of graphite into few-layer graphene platelets without damages on their basal plane for better performance. Dispersed platelets were drop-coated to produce a thin film that was then heat-treated at 600 °C under argon atmosphere, yielding a uniformly welded large-area graphene films with low sheet resistance (0.52−3.11 kΩ/sq) and comparable optical transmittance (63−90%). The EFG approach is a scalable method for the cost-effective production of high-quality graphene films.

METHODS

Materials. All reagents and solvents were purchased from Aldrich Chemical Inc., and used as received, unless otherwise mentioned. 4-Ethylbenzoic acid as a reactive molecular wedge was purified by recrystallization from heptanes (mp = 112−113 °C). Graphite (99.9% purity, stock no. 1250HT, CAS no. 7782-42-5, Lot no. 1250-100907) was obtained from Nanostructured & Amorphous Materials Inc., USA, and used as received.

Instrumentations. Raman spectra were taken with He−Ne laser (532 nm) as the excitation source by using combined AFM and confocal Raman microscope (Alpha 300S, WITec, Germany). Themogravimetric analysis (TGA) was conducted in air and nitrogen atmospheres at a heating rate of 10 and 1 °C/min using a TA Hi-Res TGA 2950 thermogravimetric analyzer. The field emission scanning electron microscopy (FE-SEM) used in this work was LEO 1530FE and FEI NanoSem 200. The field emission transmission electron microscope (FE-TEM) employed in this work was a FEI Tecnai G2 F30 S-Twin. The operating voltage was 200 kV. The samples were prepared by dispersion in *N*-methyl-2-pyrrolidone (NMP). X-ray photoelectron spectroscopy (XPS) was performed with Thermo Fisher K-alpha. Elemental analysis (EA) was conducted with Thermo Scientific Flash 2000. Atomic force microscopy (AFM) analysis was conducted with Veeco Multimode V. X-ray diffraction (XRD) patterns were recorded with Rigaku D/Max2500/PC. The field-effect transistor was fabricated by transferring the HEFG film on prepatterned electrodes, which were defined on SiO_2/Si (300 nm thick SiO_2 layer on a highly doped p-type Si(100)) substrates by addressing Cr (5 nm)/Au (20 nm) electrodes by using a conventional photolithography (photoresist: AZ7210). The channel length was 4 μm. $I-V_g$ curve of a field-effect transistor was obtained by using a semiconductor analyzer (Keithley 4200). The measurement was carried out in vacuum and bias voltage of 0.1 V between source and drain electrodes.

Procedure for the Functionalization of Graphite with 4-Ethylbenzoic Acid in Polyphosphoric Acid (PPA)/Phosphorus Pentoxide (P_2O_5). Graphite was functionalized with 4-ethylbenzoic acid (EBA) in a 250 mL resin flask equipped with a high-torque mechanical stirrer and the nitrogen inlet and outlet. Into the flask, EBA (0.5 g, 16.65 mmol), graphite-powder (0.5 g), PPA (83% P_2O_5 assay: 100.0 g) and P_2O_5 (25 g) were placed and stirred under dry nitrogen purge at 130 °C for 72 h. The initial black mixture became lighter and viscous as the functionalization onto graphite progressed. At the end of the reaction, the color of the mixture turned dark green, and water was added into the flask. The resulting tanned brown precipitate was collected by suction filtration, Soxhlet-extracted with water for 3 days to completely remove reaction medium, and then with methanol for 3 more days to get rid of unreacted EBA and low molar mass impurities. Finally, the sample was freeze-dried under reduced pressure (0.5 mmHg) at −120 °C for 72 h to give 0.58 g (60% yield) of tanned brown powder (Supporting Information, Figure S2b). Anal. Calcd. for $C_{71.57}H_9O$: C, 97.17%; H, 1.02%; O, 1.81%. Found: C, 95.71%; H, 1.03%; O, 1.59%.

The amount of EFG dispersed in each solvent was calculated as described as follows: (1) a given amount of EFG was dispersed in the solvent with magnetic stirring; (2) the dispersion was allowed to sediment overnight (12 h); (3) it was then centrifuged and the centrifuged portion and supernatant were then separated; (4) solvent was removed from the centrifuged portion; (5) the residual solid from the centrifuged portion was weighed; (6) the amount of exfoliated EFG in the supernatant was estimated by subtracting the residual weight from the centrifuged portion from the original EFG weight added in the first step.

Computation. The Vienna *Ab Initio* Simulation Package (VASP) with the Perdew−Burke−Ernzerhof version of the gradient-corrected functional was used. The projector-augmented-wave pseudopotential was employed for the atomic potential, and the plane-wave basis set was used with the energy cutoff of 400 eV.[28]

Here, a graphene fragment is modeled by the zigzag-edged graphene ribbon. The binding strength between dichloromethane solvent molecules and the ethyl-benzoyl terminal groups was calculated as shown in Supporting Information, Figure S6. The adsorption strength of the solvent molecules was found to be 14.7 kJ/mol. During delamination, the van der Waals interaction between neighboring layers in graphite competes with the attraction force between the edge-functional groups and solvent molecules. The van der Waals attraction between solvent molecules and the surface of graphene also contributes to the energetics of delamination.

Acknowledgment. This work was supported by the World Class University (WCU), US-Korea NBIT and Basic Research Laboratory (BRL) programs supported by National Research Foundation (NRF) of Korea and the US Air Force Office of Scientific Research (AFOSR).

Supporting Information Available: Experimental procedure, digital photos, TGA, XPS, AFM, XRD, confocal image, Raman, model geometry, SEM and EA. This material is available free of charge *via* the Internet at http://pubs.acs.org.

REFERENCES AND NOTES

1. Lee, C.; Wei, X.; Kysar, J. W.; Hone, J. Measurement of the Elastic Properties and Intrinsic Strength of Monolayer Graphene. *Science* **2008**, *321*, 385–388.
2. Balandin, A. A.; Ghosh, S.; Bao, W.; Calizo, I.; Teweldebrhan, D.; Miao, F.; Lau, C. N. Superior Thermal Conductivity of Single-layer Graphene. *Nano Lett.* **2008**, *8*, 902–907.
3. Novoselov, K. S.; Geim, A. K.; Morozov, S. V.; Jiang, D.; Zhang, Y.; Dubonos, S. V.; Grigorieva, I. V.; Firsov, A. A. Electric Field in Atomically Thin Carbon Films. *Science* **2004**, *306*, 666–669.
4. Stankovich, S.; Dikin, D. A.; Dommett, G. H. B.; Kohlhaas, K. M.; Zimney, E. J.; Stach, E. A.; Piner, R. D.; Nguyen, S. T.; Ruoff, R. S. Graphene-Based Composite Materials. *Nature* **2006**, *442*, 282–286.
5. Stoller, M. D.; Park, S.; Yanwu, Z.; An, J.; Ruoff, R. S. Graphene-Based Ultracapacitors. *Nano Lett.* **2008**, *8*, 3498–3502.

6. Mohanty, N.; Berry, V. Graphene-Based Single-Bacterium Resolution Biodevice and DNA Transistor: Interfacing Graphene Derivatives with Nanoscale and Microscale Biocomponents. *Nano Lett.* **2008**, *8*, 4469–4476.
7. Freitag, M. Graphene: Nanoelectronics Goes Flat Out. *Nat. Nanotechnol.* **2008**, *3*, 455–457.
8. Geim, A. K.; Novoselov, K. S. The Rise of Graphene. *Nat. Mater.* **2007**, *6*, 183–191.
9. Novoselov, K. S.; Geim, A. K.; Morozov, S. V.; Jiang, D.; Katsnelson, M. I.; Grigorieva, I. V.; Dubonos, S. V.; Firsov, A. A. Two-dimensional Gas of Massless Dirac Fermions in Graphene. *Nature* **2005**, *438*, 197–200.
10. Kim, K. S.; Zhao, Y.; Jang, H.; Lee, S. Y.; Kim, J. M.; Ahn, J. H.; Kim, P.; Choi, J. Y.; Hong, B. H. Large-Scale Pattern Growth of Graphene Films for Stretchable Transparent Electrodes. *Nature* **2009**, *457*, 706–710.
11. Minami, T. Transparent Conducting Oxide Semiconductors for Transparent Electrodes. *Semicond. Sci. Technol.* **2005**, *20*, S35–S44.
12. Bae, S.; Kim, H.; Lee, Y.; Xu, X.; Park, J. S.; Zheng, Y.; Balakrishnan, J.; Lei, T.; Ri Kim, H.; Song, Y. I.; *et al*. Roll-to-roll Production of 30-in. Graphene Films for Transparent Electrodes. *Nat. Nanotechnol.* **2010**, *5*, 574–578.
13. Li, X.; Cai, W.; An, J.; Kim, S.; Nah, J.; Yang, D.; Piner, R.; Velamakanni, A.; Jung, I.; Tutuc, E.; *et al*. Large-Area Synthesis of High-Quality and Uniform Graphene Films on Copper Foils. *Science* **2009**, *324*, 1312–1314.
14. De, S.; Coleman, J. N. Are There Fundamental Limitations on the Sheet Resistance and Transmittance of Thin Graphene Films? 2010, *5*, 2713-2720.
15. Hummers, W. S., Jr.; Offeman, R. E. Preparation of Graphitic Oxide. *J. Am. Chem. Soc.* **1958**, *80*, 1339.
16. Boukhvalov, D. W.; Katsnelson, M. I. Modeling of Graphite Oxide. *J. Am. Chem. Soc.* **2008**, *130*, 10697–10701.
17. Choi, E. K.; Jeon, I. Y.; Bae, S.-Y.; Shin, H. S.; Dai, L.; Baek, J. B. High-Yield Exfoliation of the Three-Dimensional Graphite into Graphene-like Sheets. *Chem. Commun.* **2010**, *46*, 6320–6322.
18. Chen, J.; Shan, J. Y.; Tsukada, T.; Munekane, F.; Kuno, A.; Matsuo, M.; Hayashi, T.; Kim, Y. A.; Endo, M. The Structural Evolution of Thin Multiwalled Carbon Nanotubes during Isothermal Annealing. *Carbon* **2007**, *45*, 274–280.
19. Stankovich, S.; Piner, R. D.; Chen, X.; Wu, N.; Nguyen, S. T.; Ruoff, R. S. Stable Aqueous Dispersions of Graphitic Nanoplatelets *via* the Reduction of Exfoliated Graphite Oxide in the Presence of Poly(sodium 4-styrenesulfonate). *J. Mater. Chem.* **2006**, *16*, 155–158.
20. Suslick, K. S. Sonochemistry. *Science* **1990**, *247*, 1439–1445.
21. Hernandez, Y.; Nicolosi, V.; Lotya, M.; Blighe, F. M.; Sun, Z.; De, S.; McGovern, I. T.; Holland, B.; Byrne, M.; Gun'ko, Y. K.; *et al*. High-Yield Production of Graphene by Liquid-Phase Exfoliation of Graphite. *Nat. Nanotechnol.* **2008**, *3*, 563–568.
22. Li, X.; Wang, H.; Robinson, J. T.; Sanchez, H.; Diankov, G.; Dai, H. Simultaneous Nitrogen Doping and Reduction of Graphene Oxide. *J. Am. Chem. Soc.* **2009**, *131*, 15939–15944.
23. Blake, P.; Hill, E. W.; Castro Neto, A. H.; Novoselov, K. S.; Jiang, D.; Yang, R.; Booth, T. J.; Geim, A. K. Making Graphene Visible. *Appl. Phys. Lett.* **2007**, 91.
24. Stolyarova, E.; Kwang, T. R.; Ryu, S.; Maultzsch, J.; Kim, P.; Brus, L. E.; Heinz, T. F.; Hybertsen, M. S.; Flynn, G. W. High-Resolution Scanning Tunneling Microscopy Imaging of Mesoscopic Graphene Sheets on an Insulating Surface. *Proc. Natl. Acad. Sci. U.S.A.* **2007**, *104*, 9209–9212.
25. Gao, W.; Alemany, L. B.; Ci, L.; Ajayan, P. M. New Insights into the Structure and Reduction of Graphite Oxide. *Nat. Chem.* **2009**, *1*, 403–408.
26. Park, S.; Ruoff, R. S. Chemical Methods for the Production of Graphenes. *Nat. Nanotechnol.* **2009**, *4*, 217–224.
27. Heersche, H. B.; Jarillo-Herrero, P.; Oostinga, J. B.; Vandersypen, L. M. K.; Morpurgo, A. F. Bipolar Supercurrent in Graphene. *Nature* **2007**, *446*, 56–59.
28. Kresse, G.; Furthmüller, J. Efficient Iterative Schemes for *ab Initio* Total-Energy Calculations Using a Plane-Wave Basis Set. *Phys. Rev. B* **1996**, *54*, 11169–11186.